Delay-Compound-Compensation Control for Photoelectric Tracking System Based on Improved Smith Predictor Scheme

Luo, Yong; Xue, Wenchao; He, Wei; Nie, Kang; Mao, Yao; Guerrero, Josep M.

Published in:
IEEE Photonics Journal

DOI (link to publication from Publisher):
10.1109/JPHOT.2022.3164202

Publication date:
2022

Document Version
Publisher's PDF, also known as Version of record

Delay-Compound-Compensation Control for Photoelectric Tracking System Based on Improved Smith Predictor Scheme

Yong Luo, Wenchao Xue, *Member, IEEE*, Wei He, *Member, IEEE*, Kang Nie, Yao Mao, *Member, IEEE*, and Josep M. Guerrero, *Fellow, IEEE*

***Abstract*—High control bandwidth is usually restricted in a photoelectric tracking system (PTS) based on a Charge-Couple Device(CCD) with time delay, which hinders a good tracking performance. Generally, a model-based delay-compensation controller called Smith predictor (SP) can help increase the controller gain to promote the bandwidth by separating delay from the control loop. However, the performance promotion is insufficient because the delay still stays in the forward channel which causes errors between output and input. And the increase of the controller gain is still limited due to the effect of model mismatch on stability. In this paper, to solve the problems, a delay-compound-compensation control (DCCC) based on improved SP by trajectory prediction and velocity feedforward is proposed. The additional trajectory prediction is used to further eliminate the effect of delay existing in the forward channel. The additional velocity feedforward is used to further reform the transfer characteristics limited by the controller gain. A Kalman filter-based design method of trajectory prediction is presented and the optimal design principle of feedback and feedforward controllers is given in the face of model mismatch. Experiments demonstrate that the DCCC is valid and could greatly promote the tracking performance in the low frequency.**

***Index Terms*—Smith predictor, time delay, charge-couple device, delay-compound-compensation, trajectory prediction, velocity feedforward.**

I. Introduction

THE photoelectric tracking system (PTS) based on a charge-coupled device (CCD) can be applied in astronomical observation, surveillance, and laser communication [1]–[4]. Sensors such as CCD provide the tracking error for control and play important roles in both orientation and tracking, because there is only error information available instead of the target's motion states [5], [6]. High bandwidth usually means good tracking performance for PTS [7]–[9]. However, relatively long time of imaging is needed to acquire a clear image for extracting a boresight error, which brings a low-sampling rate and inevitable time delay to the system. Delay leads to phase attenuation, which limits the system bandwidth and causes the tracking performance degradation [10]. To compensate for the negative influence of delay, scholars have adopted many optimization schemes, which are mainly divided into two categories.

One effective way is to level up the system's control type. A PID-I control [11] and a fractional order control [12] are proposed to decrease the steady-state error of the system. But they would sacrifice parts of the system stability and dynamic performance. A feedforward control which can improve the control type equivalently is used to enhance the performance of delayed systems [13], [14]. Since the target information in PTS is not measurable, the current target state used for feedforward is obtained by a trajectory prediction method based on a synthesized trajectory in the past time [15], [16]. However, this kind of feedforward method requires additional sensors and its control performance decreases significantly as the frequency increases.

Different from the strategy of increasing the system type, a model-based delay-compensation method widely used in industry, also known as Smith predictor (SP) can increase the controller gain to promote the bandwidth without additional sensors [17]–[19]. SP succeeds in its simplicity. It uses the output of the system's model to make feedback in advance, which can improve the system's reaction speed by approximately excludes the effect of delay on stability. Over past few decades, many modifications of the SP have been reported to facilitate the tuning and improve the robustness for industrial processes [20]–[22]. A modified SP controller with two degrees of freedom is proposed to decouple the set point responses from the load disturbances responses for integration processes with delay [23]. In case of model mismatch, a strict bound on the controller gain is derived with a geometrical analysis approach [24]. In order to make up for the lack of performance of SP in systems with varying delays, an adaptive SP based on a delay measured in real time is proposed [25]. Although the research on SP started very early, its application in PTS began in just recent years. An improved SP based on a closed-loop model is firstly introduced to the

Manuscript received November 21, 2021; revised January 11, 2022; accepted March 29, 2022. Date of publication April 1, 2022; date of current version April 28, 2022. *(Corresponding author: Yao Mao.)*

Yong Luo and Wei He are with the Nanjing University of Information Science and Technology, Nanjing, Jiangsu 210044, China (e-mail: luoyong@nuist.edu.cn; hwei@nuist.edu.cn).

Wenchao Xue is with the LSC, NCMIS, Academy of Mathematics and Systems Science, Chinese Academy of Sciences, Beijing 100190, China, and also with the School of Mathematical Sciences, University of Chinese Academy of Sciences, Beijing 100049, China (e-mail: wenchaoxue@amss.ac.cn).

Kang Nie and Yao Mao are with the Key Laboratory of Optical Engineering, Institute of Optics and Electronics, Chinese Academy of Science, University of Chinese Academy of Sciences, Beijing 101408, China (e-mail: kangnie@outlook.com; maoyao@ioe.ac.cn).

Josep M. Guerrero is with the Department of Energy Technology, Aalborg University, DK-9220 Aalborg, Denmark (e-mail: joz@et.aau.dk).

Digital Object Identifier 10.1109/JPHOT.2022.3164202

PTS to compensate its small delay with stronger robustness [26]. A technique of modified SP is introduced in the visual servomechanism wherein the output of a mathematical model is replaced by an integration of the gyroscope's signal from the inner loop, which can reduce dependence on the model [27]. In order to increase the anti-disturbance ability of the visual axis while compensating for the time delay, an enhanced SP with disturbance observation function is proposed [28]. However, despite these improvements, its inherent problems still exist. Firstly, although both the original and improved SP can reduce the effect of delay on stability by separating it from the loop, delay still stays in the forward channel, resulting in errors between output and input. Secondly, the bandwidth of the system cannot be increased too much, because the existed mismatch between the plant and its model will still limit the gain for stability reasons, resulting in unsatisfactory transfer characteristics.

In this paper, to solve the problems, a delay-compound-compensation control(DCCC) based on improved SP by trajectory prediction and velocity feedforward is proposed. The additional trajectory prediction is used to further eliminate the effect of delay existing in the forward channel. The additional velocity feedforward is used to further reform the transfer characteristics limited by controller gain. A Kalman filter-based design method of trajectory prediction is presented and the optimal design principle of feedback and feedforward controllers is given in the face of model mismatch. Although both the proposed trajectory prediction and velocity feedforward commonly work at low frequencies, it meets the performance needs because the target signal is mainly concentrated in this spectrum. Series of experiments demonstrate that the proposed DCCC is valid and could greatly promote the tracking performance in the low frequency.

The main contributions of this paper can be summarized as follows:

i) An additional trajectory prediction link is added to the classic SP method to further eliminate the effect of delay existing in the forward channel.
ii) An additional velocity feedforward branch is added to the SP to further reform the transfer characteristics restricted by the limited controller gain.
iii) The optimal design principle of feedback and feedforward controllers is given in the face of the model mismatch existed in the system.

This paper is organized as below. Section II presents a detailed introduction of the CCD-based PTS, mainly describing the system structure, the SP's principle and its bottlenecks. Section III gives out the structure of the DCCC and discusses its promotion for tracking performance. Section IV gives the design of Kalman filter to predict the current trajectory. Section V demonstrates the system stability condition and provides the optimal parameters selection. Section VI sets up a list of experiments to confirm the effectiveness of DCCC. Concluding remarks are presented in Section VII.

II. Problem Formulation

The configuration of the CCD-based PTS is illustrated in Fig. 1. The light of the target is imaged on a CCD through the lens and the image processing unit extracts the boresight error. The servo control unit accepts the error to calculate the control amount and implement a closed loop. The driver actuates the motors to accomplish the tracking process. In addition, a gyroscope is commonly added to suppress the parameter perturbation of the platform, which constructs a basic dual-loop control mode with the outer position loop.

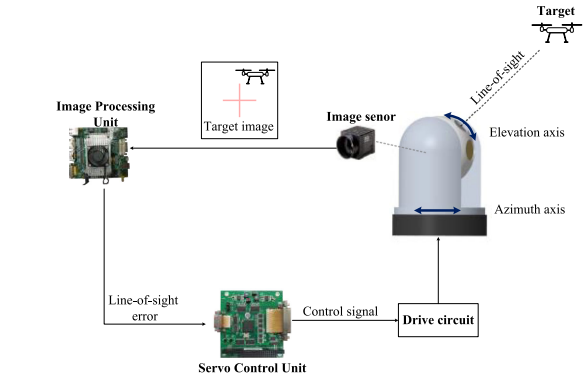

Fig. 1. The configuration of the PTS.

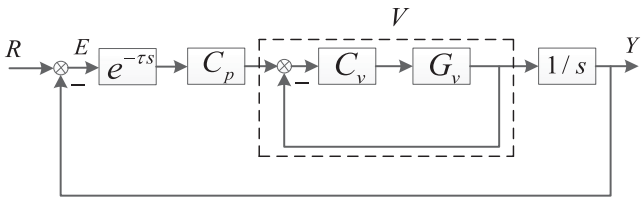

Fig. 2. The dual-loop control structure of the PTS.

The dual-loop control structure of the PTS is presented in Fig. 2. G_v is the control plant. C_v, C_p respectively refers to the velocity controller and position controller. $e^{-\tau s}$ refers to the transfer function of the CCD though it may be rough without considering signal attenuation and nonlinearity, where τ is the delay time. E is the boresight error. R refers to the target signal. Y refers to the corresponding movement of the plant. For the control system of PTS, the error transfer function (ETF), that is, the ratio of the error to the target position, is the most important index to evaluate its performance. The ETF of the dual-loop control is exhibited as (1).

$$S_0 = \frac{E}{R} = \frac{1}{1 + C_p V \frac{1}{s} e^{-\tau s}}. \tag{1}$$

$V = C_v G_v / (1 + C_v G_v)$ is the velocity closed-loop transfer function. Because of the high bandwith of the inner loop, $V \approx 1$ is reasonable in a wide frequency range. Then, the position controlled object is transformed into a first-order integral system and S_0 can be simplified to $S_0 \approx 1/(1 + C_p e^{-\tau s}/s)$. Due to the lag effect of delay on the phase, the control gain is usually limited to a small amount to ensure the system's stability, resulting in a very low control bandwidth.

To reduce the effect of delay on the bandwidth, a classic SP based on a simple integral model is added to the dual-loop system shown as Fig. 3. The dotted frame is the SP structure, in which

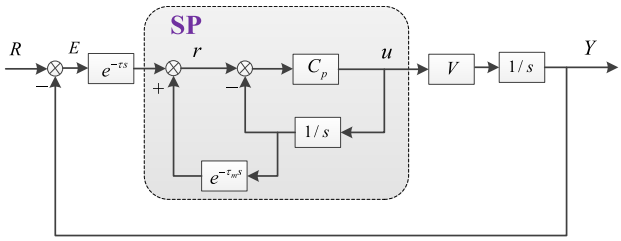

Fig. 3. The control structure of the SP.

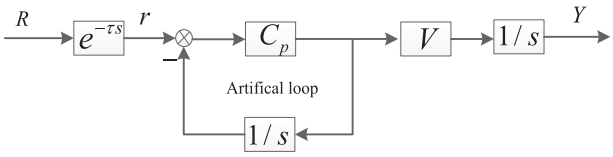

Fig. 4. The approximately equivalent structure of the SP.

τ_m is the estimation of τ. The ETF in Fig. 3 is exhibited as (2).

$$S_{SP} = \frac{E}{R} = \frac{1 + C_p\frac{1}{s}(1 - e^{-\tau_m s})}{1 + C_p\frac{1}{s} + C_p\frac{1}{s}\left(Ve^{-\tau s} - e^{-\tau_m s}\right)}. \quad (2)$$

Since $V \approx 1$ and $\tau \approx \tau_m << 1$, S_{SP} can be simplified as $S_{SP} \approx [1 + C_p\frac{1}{s}(1 - e^{-\tau s})]/(1 + C_p\frac{1}{s})$ in a wide frequency band, in which the effect of delay on stability is greatly reduced if the model is accurate. For a more intuitive explanation, we give its approximately equivalent structure in Fig. 4. As we can see, delay is equivalent to being separated from the artifical loop, which would reduce the restrictions on the controller, giving the system a higher bandwidth with better performance.

However, it must be pointed out that the performance improvement brought by SP is still insufficient. First of all, since the delay separated by SP still exists in the forward channel which can be seen from Fig. 4, the output cannot track the input in time, resulting in bigger errors. In addition, the gain of the controller in SP cannot be increased indefinitely, because such matching between the plant and the model can seldom be achieved in practice. In other words, the control structure of the SP in Fig. 4 still do not have an ideal transmission characteristics, which still limits the performance improvement. Considering the above two factors, we know that the tracking performance of the PTS with SP still has a lot of room for improvement.

III. The DCCC Method

In order to comprehensively improve the tracking performance of the PTS with SP, a DCCC method is proposed, which simultaneously adds a trajectory prediction link and a velocity feedforward branch into the SP structure, as shown in Fig. 5. Q is a state estimator with predictive function. It can estimate the current state of the target to further eliminate the effect of delay existing in the forward channel. The additional velocity feedforward can further improve the suboptimal transfer characteristics of the delay-free artificial loop in Fig. 4. F is a feedforward controller designed to ensure stability.

Before using the estimator Q for trajectory prediction, we need to examine the characteristics of its input signal. The

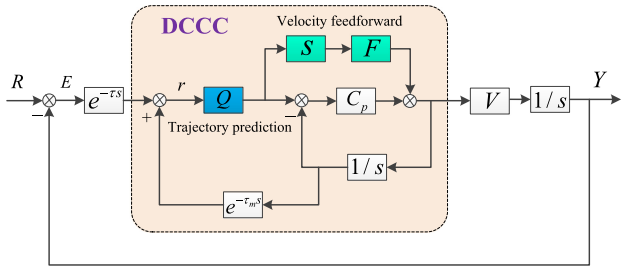

Fig. 5. The control structure of the DCCC.

expression of the intermediate signal r before adding improvements is as

$$r = \frac{R \cdot e^{-\tau s} \cdot \left(1 + C_p\frac{1}{s}\right)}{1 + C_p\frac{1}{s} + C_p\frac{1}{s}\left(Ve^{-\tau s} - e^{-\tau_m s}\right)}. \quad (3)$$

Similarly, $r \approx R \cdot e^{-\tau s}$ can be easily concluded in the frequency of most concern. In other words, we can obtain the past trajectory of the target through SP, unlike traditional feedforward control, which requires additional sensors to help synthesize the trajectory [15]. Based on it, we can predict the current trajectory to eliminate the effect of the delay with a trajectory prediction method. In addition, the velocity feedforward can perfectly compensate the feedback control since all the parameters of the artificial loop are deterministic. To examine the effect of the DCCC on performance, the ETF in Fig. 5 is given as

$$S_{DCCC} = \frac{E}{R} = \frac{(1 - Fe^{-\tau_m s}Q) + C_p\frac{1}{s}(1 - e^{-\tau_m s}Q)}{1 + C_p\frac{1}{s} + \left(C_p\frac{1}{s} + F\right)Q\left(Ve^{-\tau s} - e^{-\tau_m s}\right)}. \quad (4)$$

Now, let's focus on the comparison of the ETFs between the SP and the DCCC. If Q has the prediction ability, $Q = e^{\tau_m s}$ is reasonable in the effective frequency band. Considering that in low frequency $V \approx 1$, $e^{-\tau_m s} \approx e^{-\tau s} \approx 1 - \tau_m s$, $F \approx 1$ and C_P can be taken as a proportional controller, the following result can be concluded:if $s \to 0$, $|S_{SP}| \to \frac{1 + C_p\tau_m}{|1 + C_p\frac{1}{s}|}$ and $|S_{DCCC}| \to 0$. Obviously, $|S_{DCCC}| < |S_{SP}|$ is easy to get, which means that the proposed DCCC can greatly improve the tracking precision and almost completely eliminate the negative impact of delay on the system in low frequency. Next, we will discuss the design of trajectory prediction and the design of the controllers with stability demand.

IV. Trajectory Prediction By Kalman Filter

As shown in (5), the total delay is composed of three main delays in the CCD-based posotion loop: τ_{CCD} refers to the image processing time, $\tau_{process}$ represents the time of data transmission, and τ_{sample} refers to the time delay of sampling. Generally, the total delay can be measured by system identification.

$$\tau = \tau_{CCD} + \tau_{process} + \tau_{sample}. \quad (5)$$

In PTS, the idea of trajectory prediction to compensate for delay starts with the traditional feedforward tracking, in which the most used trajectory prediction method is Kalman filter. Kalman filter succeeds in its low computational complexity and high

precision, and researchers have proposed many improved algorithms, such as extended Kalman filter [29], unscented Kalman filter [30], and many others [31]. In addition, the combination of Kalman filter with adaptive structure, robust control, etc. is also widely used [32], [33]. Considering that the PTS can be regarded as a linear system, and the main goal of this paper is to verify the effectiveness of the DCCC structure, it is sufficient in this paper to select a linear Kalman filter to predict the target position. Since the two axes of the PTS are symmetrical, this section only focuses on the signal prediction in one axe. Firstly, the state equation and measurement equation of the target are given as (6). x_k is the motion state vector of the target including position, velocity and acceleration. The observed signal r_k is the trajectory at the past moment recovered by the boresight error and the output of the model. w_{k-1} represents the process noise and v_k represents the observation noise, which are both Gaussian white noise with $w_{k-1} \sim N(0, I_{k-1})$ and $v_{k-1} \sim N(0, J_k)$. A is the state-transition matrix, G is the input matrix of the process noise and C is the observation matrix.

$$\begin{cases} x_k = Ax_{k-1} + Gw_{k-1} \\ r_k = Cx_k + v_k \end{cases}. \tag{6}$$

The coefficient matrixs of the above state equation and observation equation is determined by two factors, one is to follow the actual movement of the target, and the second is to facilitate calculation. Under normal circumstances, there is little prior experience of the target movement, and there are many uncertainties in the maneuvering state. Therefore, approximate processing is widely adopted under some assumptions. Generally, commonly used models include uniform acceleration model, Singer model, current statistical model and interactive multi-model structure [34]–[36]. In theory, all of these motion models for different scenarios can be used to verify the effectiveness of DCCC. However, since the DCCC structure is mainly used to improve the low-frequency performance of the system and focus on the non-strong maneuvering characteristics of the target, this paper chooses a uniform acceleration model with less computational complexity and suitable for low-frequency signals prediction. Then the parameters of the Kalman filter can be easily known as follows, in which T is the sampling frame.

$$\begin{aligned} A &= \begin{bmatrix} 1 & T & 0.5T^2 \\ 0 & 1 & T \\ 0 & 0 & 1 \end{bmatrix} \\ G &= \begin{bmatrix} \frac{1}{6}T^3 & \frac{1}{2}T^2 & T \end{bmatrix}^T \\ C &= \begin{bmatrix} 1 & 0 & 0 \end{bmatrix}. \end{aligned} \tag{7}$$

The one-step prediction equation for estimating the target state is

$$x_{k|k-1} = Ax_{k-1|k-1}. \tag{8}$$

The covariance matrix of one-step prediction is

$$P_{k|k-1} = AP_{k-1|k-1}A^T + GI_{k-1}G^T. \tag{9}$$

The Kalman filter gain is

$$K_k = P_{k|k-1}C^T \left[CP_{k|k-1}C^T + J_k \right]^{-1}. \tag{10}$$

The update of the target's motion state is

$$x_{k|k} = x_{k|k-1} + K_k \left[r_k - Cx_{k|k-1} \right]. \tag{11}$$

The update of the covrariance matrix is

$$P_{k|k} = \left[I - K_k C \right] P_{k|k-1}. \tag{12}$$

Commonly, Kalman filter exhibits a low-pass characteristic, which means that the prediction usually only works at low frequencies. Since r_k contains delay, the trajectory corrected by (11) is at the past time. To get the current trajectory, iterative calculations need to be performed according to (8) and the number of iterations is determined by the ratio of the total delay to the sampling period. [33] shows that the larger the ratio of the variance I_{k-1} of the process noise to the variance J_k of the observation noise, the higher the bandwidth. However, an unreasonable high bandwidth will cause waveform distortion, so usually the bandwidth of Kalman filter is limited to a small range.

V. Controller Design Based on Stability Analysis

This section analyzes the stability and robust stability conditions, and provides criterions for the design of the controller parameters. When using the DCCC method, the ETF in (4) can be rewritten as

$$S_{DCCC} = \frac{E}{R} = \frac{(1 - Fe^{-\tau_m s}Q) + C_p \frac{1}{s}(1 - e^{-\tau_m s}Q)}{\left(1 + C_p \frac{1}{s}\right)\left[1 + \frac{\left(C_p \frac{1}{s} + F\right)Q(Ve^{-\tau s} - e^{-\tau_m s})}{1 + C_p \frac{1}{s}}\right]}. \tag{13}$$

Because the left term $(1+C_p \frac{1}{s})$ in the denominator of S_{DCCC} is the characteristics polynomial of a first-order integral system that must be stable, the stability condition of this DCCC system has to meet the following equation according to the small-gain theorem.

$$\left\| \frac{\left(C_p \frac{1}{s} + F\right) Q \left(Ve^{-\tau s} - e^{-\tau_m s}\right)}{1 + C_p \frac{1}{s}} \right\|_\infty < 1. \tag{14}$$

In low frequency, Q has predicting function that can be approximately represented by $e^{\tau_m s}$. In high frequency, it has no predict function and its amplitude is generally not greater than 1. Therefore, a relatively conserved condition for stability can be

$$\left\| \frac{\left(C_p \frac{1}{s} + F\right) \left(Ve^{-\tau s} - e^{-\tau_m s}\right)}{1 + C_p \frac{1}{s}} \right\|_\infty < 1. \tag{15}$$

Since both the SP and the DCCC are model-based control methods, the design of the controller needs to consider the situation of model mismatch. Considering that the velocity loop has a high bandwidth with strong robustness, the model mismatch mainly comes from the delay mismatch. That is, the case where $\tau \neq \tau_m$. Since the position object is an integral link, C_p can be selected as a proportional controller represented by k , and F can be selected as a first-order low-pass filter $1/(1 + Ts)$. Then, substitute $C_p = k$, $F = 1/(1 + Ts)$, $V = 1$ and $s = j\omega$

into (15), we get a condition for any ω as

$$\left| \frac{k + \frac{j\omega}{1+Tj\omega}}{j\omega + k} \left(e^{-j\tau\omega} - e^{-j\tau_m\omega} \right) \right| < 1. \tag{16}$$

Assuming that $\Delta\tau = \tau_m - \tau$ is the delay uncertainty, after calculation, Equations (16) turns out to be

$$1 - \frac{\left(1 + T^2\omega^2\right)\left(k^2+\omega^2\right)}{k^2 + (kT+1)^2\omega^2} \cdot \frac{1}{2} \leq \cos\left(\omega\Delta\tau\right). \tag{17}$$

Since $\frac{1}{(kT+1)^2} \leq \frac{k^2+\omega^2}{k^2+(kT+1)^2\omega^2} \leq 1$, Equation (17) changes to

$$f_1\left(\omega\right) = 1 - \frac{\left(1 + T^2\omega^2\right)}{\left(kT+1\right)^2} \cdot \frac{1}{2} \leq \cos\left(\omega\Delta\tau\right) = f_2\left(\omega\right). \tag{18}$$

A sufficient condition for (18) is

$$\left| \frac{df_2\left(\omega\right)}{d\omega} \right| \leq \left| \frac{df_1\left(\omega\right)}{d\omega} \right|, \tag{19}$$

which turns out the condition $\frac{T^2\omega}{(kT+1)^2} \geq \Delta\tau \sin(\omega\Delta\tau)$. This condition can be satisfied if

$$\left| \frac{df_2^2\left(\omega\right)}{d\omega^2} \right| \leq \left| \frac{df_1^2\left(\omega\right)}{d\omega^2} \right|. \tag{20}$$

Then, we get

$$k + \frac{1}{T} \leq \frac{1}{\Delta\tau\sqrt{\left|\cos\left(\omega\Delta\tau\right)\right|}}. \tag{21}$$

Finally, it can be concluded that the following condition should be satisfied to get asymptotic stability.

$$k + \frac{1}{T} \leq \frac{1}{\Delta\tau}. \tag{22}$$

The stability condition (22) expresses a trade-off between the delay uncertainty $\Delta\tau$ and the parameters of the controllers that can be used to tune the controller gain k and the time constant T. If $1/T \to 0$, it means that the velocity feedforward does not exist and we can actually deduce that the stability condition of the classic SP is $k \leq 1/\Delta\tau$. Regarding how to choose the values of k and T to get the optimal error suppression capability, we need pay attention to the ETF in (4) again.

Considering that $V \approx 1$, $e^{-\tau s} \approx e^{-\tau_m s}$ and $Q = e^{\tau_m s}$ in a relatively wide frequency range, we substitute $F = 1/(1+Ts)$ and $C_p = k$ into (4), geting its simplified form of low-frequency as

$$S_{DCCC} \approx \frac{1 - F}{1+C_p\frac{1}{s}} = \frac{s^2}{s^2 + \left(k + \frac{1}{T}\right)s + \frac{k}{T}}. \tag{23}$$

Let $s = j\omega$, we get its amplitude as

$$\left|S_{DCCC}\right| \approx \frac{\omega^2}{\sqrt{\omega^2\left(k + \frac{1}{T}\right)^2 + \left(\frac{k}{T} - \omega^2\right)^2}}. \tag{24}$$

It can be seen that the larger the denominator, the smaller the sensitivity transfer function and the higher the tracking precision. According to the stability condition (22), $k + 1/T = 1/\Delta\tau$ should be chosen to obtain the strongest error suppression capability. Then we examine the value of the following formula

$$L = \left(\frac{k}{T} - \omega^2\right)^2, \tag{25}$$

where $T \geq \Delta\tau$. When $\omega < \sqrt{k/T}$, the bigger k/T is, the bigger L is and the performance is better. However, when $\omega > \sqrt{k/T}$, the smaller k/T is, the bigger L is. It means that the value of k/T has opposite effects on low-frequency and high-frequency performance. Generally speaking, since the target signal is mainly concentrated in the low frequency area for the PTS, the low-frequency performance is more important than the high-frequency performance. Therefore, it is reasonable to use the low-frequency performance as the criterion for the parameters of controllers.

Obviously, when $k = \frac{1}{T} = \frac{1}{2\Delta\tau}$, k/T gets the maximum value. Compared with any situation where $k = a$ and $T = b$, L gets bigger value when $k = \frac{1}{T} = \frac{1}{2\Delta\tau}$ for $\omega \leq m = \frac{\sqrt{a/b}+1/(2\Delta\tau)}{2}$. Since $m \geq \frac{1}{4\Delta\tau}$, it can be concluded that when $k = \frac{1}{T} = \frac{1}{2\Delta\tau}$, the system has the optimal tracking performance for $\omega \leq \frac{1}{4\Delta\tau}$.

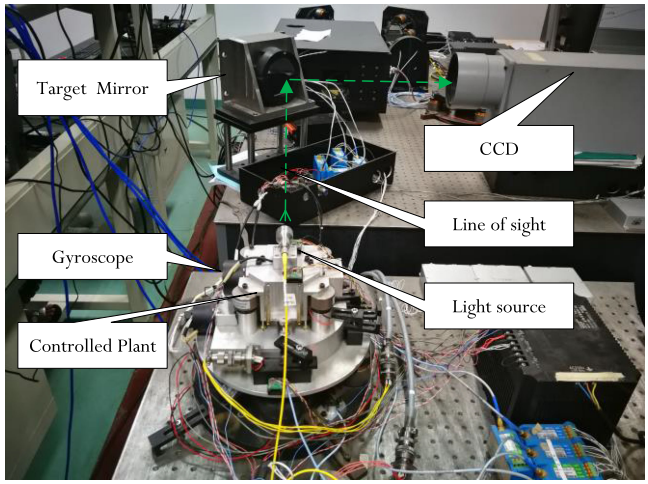

Fig. 6. Experimental setup.

VI. Experimental Verification

To verify the effectiveness of the DCCC method, an experimental setup implementing the PTS is exhibited in Fig. 6. There are two deflection devices driven by voice coil motors. One is the controlled plant for tracking, the other is called the target mirror for simulating target motion. Light ray is generated by a laser and it is reflected from the target mirror to the CCD.The image proccessing unit calculates the position error to help control the plant. A high-performance fiber-optics gyroscope is used to sense the rotating rate to implement the velocity closed loop. The CCD works at 50 Hz with an artificially added delay(one frame). The gyroscope works at 5000 Hz.

The open-loop and closed-loop velocity bode responses are exhibited in Fig. 7. Through system identification, the open-loop

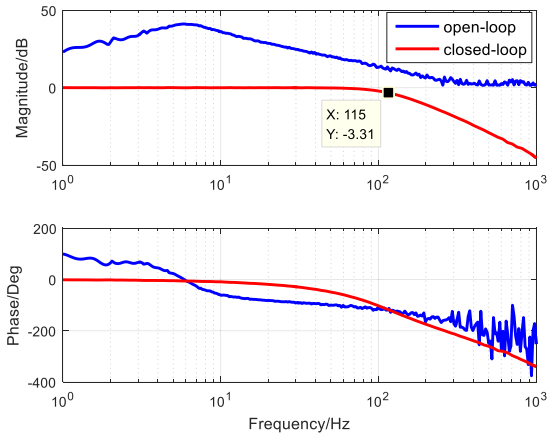

Fig. 7. The frequency responses of the velocity characteristic.

transfer function can be obtained as

$$\tilde{G}_v(s) = \frac{2.3s}{0.00072s^2 + 0.0202s + 1} \cdot \frac{1}{0.0005s + 1}. \quad (26)$$

There is a resonance peak at 7 Hz in the open-loop bode response which is not conductive to the controller design of the position loop. Therefore, a gyro-assisted velocity loop is firstly used to transform the transfer characteristics. In the velocity closed-loop bode response, the resonance has been eliminated with a bandwidth of over 100 Hz, so $V \approx 1$ is reasonable in a wide frequency domain. Then, the position object of the system can be treated as an integral process companied by delay with $\tilde{G}_p = \frac{V}{s} e^{-\tau s} \approx \frac{e^{-0.02s}}{s}$.

Generally, the model error of the time delay can be roughly obtained by measuring in advance according to the different background complexity. In this experiment, the uncertainty of the delay is set to 50%. Before adding DCCC, the position controller of the classic SP can be designed as $C_p = 1/\Delta\tau = 1/(\tau \cdot 50\%) = 100$ according to the SP's stability condition. For the DCCC structure, according to the optimal parameters conditions, the parameters of the feedback and feedforward controllers can be designed as $k = \frac{1}{T} = 50$.

The Kalman filter prediction is designed according to the steps described previously. The variance of the process noise and the variance of the observation noise are respectively selected as $I_{k-1} = 1$ and $J_k = 0.01$. In order to verify the prediction effect, Fig. 8 shows the comparison of different frequency signals before and after prediction. Below 1 Hz, the phase attenuation of the synthesized signal r is compensated well and the signal after prediction almost coincides with the reference signal. In 2 Hz, the phase attenuation can only be compensated partially, but it will also bring a slight distortion of the amplitude. It means that the method of trajectory prediction is more suitable for use in low frequency bands.

To illustrate the advantages of the proposed DCCC over the SP, several characteristic curves of the ETF with different ways are shown in Fig. 9. It can be seen that although the classic SP control can improve the tracking performance in the low-frequency band compared with the dual-loop control, the improvement is still insufficient. When the trajectory prediction

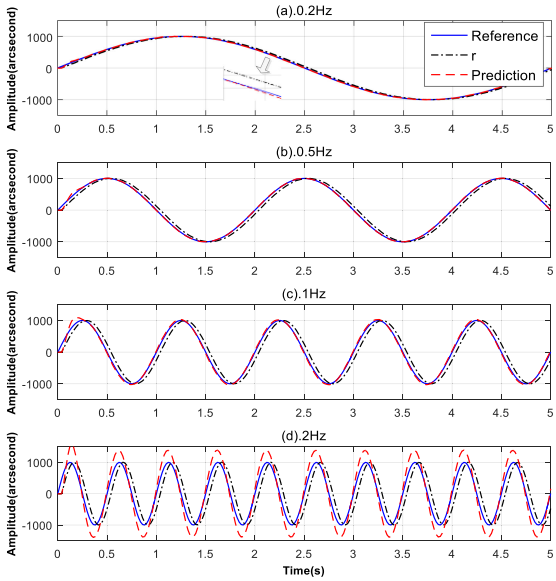

Fig. 8. The trajectory signal before and after prediction.

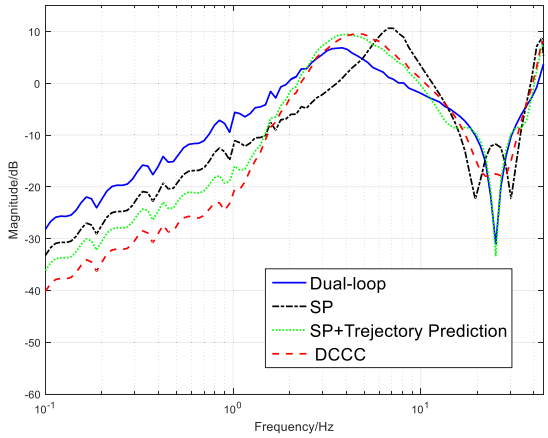

Fig. 9. The comparison of the error transfer characteristics.

is added, the tracking performance of the system within the bandwidth of Kalman filter is significantly improved. The deterioration of the high-frequency tracking performance is caused by the poor performance of the trajectory prediction in this frequency range. After the velocity feedforward is added to the system to form the DCCC method, the tracking performance is significantly improved below 4Hz, which is consistent with the calculated optimal frequency band $\omega \leq \frac{1}{4\Delta\tau \cdot 2\pi} \approx 3.98$Hz. In summary, compared with SP, the DCCC method could greatly improve the low-frequency tracking performance. Although the performance of some high-frequency bands has deteriotated, it is still acceptable because signals concentrate on low frequencies and the loss of high frequency performance is relatively small.

Fig. 10 exhibits the comparision of the time-domain residual errors in different frequencies between the classical SP and the proposed DCCC. Obviously, the accuacy of the system with DCCC is higher than it with SP at low frequencies, which is completely consistent with the above frequency-domain analysis. Figs. 11 and 12 show the trajectories and errors of tracking

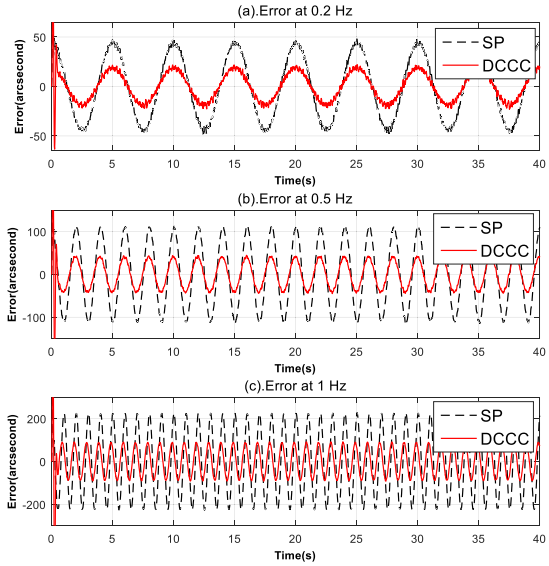

Fig. 10. The comparison of residual tracking errors in different frequencies.

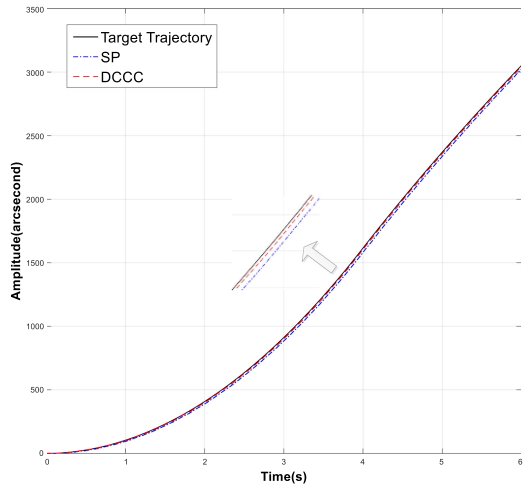

Fig. 11. The tracking trajectories with different methods.

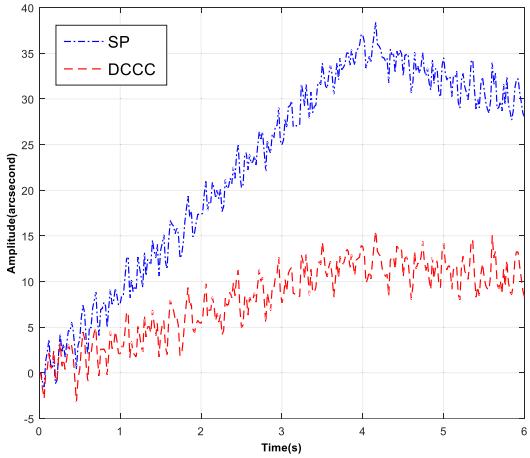

Fig. 12. The tracking errors with different methods.

a maneuvering target on one axis with SP and DCCC methods, respectively. Obviously, after adopting the DCCC method, the tracking ability has been greatly enhanced, and the tracking error has been significantly reduced.

VII. Conclusion

This paper proposes a DCCC method based on an improved SP scheme by trajectory prediction and velocity feedforward. Different from the classic SP control which can partially promote the system's control performance by separating delay from the loop, the proposed DCCC can not only continue to eliminate the effect of the separated delay, but also improve the system's transfer characteristics to the greatest extent. That is, the proposed DCCC controller approximately completely compensates the negative impact of the delay on the system, and maximizes the tracking performance of the system. Experiments show that DCCC can greatly improve the tracking accuracy in the low frequency domain where the target signal is mainly concentrated. Since this method is only based on simple models and is esay to implement, it also has a good application prospect in other industrial control with time delay. The combination of SP and multiple feedforward is promising and challenging for our next work.

References

[1] Q. Dong, Y. Liu, Y. Zhang, S. Gao, and T. Chen, "Improved ADRC with ILC control of a CCD-based tracking loop for fast steering mirror system," *IEEE Photon. J.*, vol. 10, no. 4, Aug. 2018, Art. no. 6601314.

[2] Y. Zhang *et al.*, "Fuzzy-PID control for the position loop of aerial inertially stabilized platform," *Aerosp. Sci. Technol.*, vol. 36, pp. 21–26, Mar. 2014.

[3] M. K. Masten, "Inertially stabilized platforms for optical imaging systems," *IEEE Control Syst. Mag.*, vol. 28, no. 1, pp. 47–64, Feb. 2008.

[4] Z. Hurak and M. Rezac, "Image-based pointing and tracking for inertially stabilized airborne camera platform," *IEEE Trans. Control Syst. Technol.*, vol. 20, no. 5, pp. 1146–1159, Sep. 2012.

[5] J. Deng, X. Zhou, and Y. Mao, "On vibration rejection of nonminimum-phase long-distance laser pointing system with compensatory disturbance observer," *Mechatronics*, vol. 74, no. 7540, Feb. 2021, Art. no. 102490.

[6] D. J. Henry *et al.*, "Line-of-sight kinematics and corrections for fast-steering mirrors used in precision pointing and tracking systems," *Int. Soc. Opt. Photon.*, vol. 9076, Jun. 2014, Art. no. 90760F.

[7] J. Tian, W. Yang, Z. Peng, and T. Tang, "Inertial sensor-based multiloop control of fast steering mirror for line of sight stabilization," *Opt. Eng.*, vol. 55, no. 11, Jul. 2016, Art. no. 111602.

[8] F. Wang, R. Wang, E. Liu, and W. Zhang, "Stabilization control mothed for two-axis inertially stabilized platform based on active disturbance rejection control with noise reduction disturbance observer," *IEEE Access*, vol. 7, pp. 99521–99529, Jul. 2019.

[9] T. Tang, T. Yang, B. Qi, G. Ren, and Q. Bao, "Error-based feedforward control for a charge-coupled device tracking system," *IEEE Trans. Ind. Electron.*, vol. 66, no. 10, pp. 8172–8180, Oct. 2019.

[10] T. Tang, B. Qi, and T. Yang, "Youla–Kucera parameterization-based optimally closed-loop control for tip–tilt compensation," *IEEE Sensors J.*, vol. 18, no. 15, pp. 6154–6160, Aug. 2018.

[11] T. Tang, J. Ma, and G. Ren, "PID-I controller of charge coupled device–based tracking loop for fast-steering mirror," *Opt. Eng.*, vol. 50, no. 4, Apr. 2011, Art. no. 043002.

[12] X. Zhou, Y. Mao, C. Zhang, and Q. He, "A comprehensive performance improvement control method by fractional order control," *IEEE Photon. J.*, vol. 10, no. 5, Oct. 2018, Art. no. 7906811.

[13] M. Boerlage *et al.*, "Model-based feedforward for motion systems," *Brain Res.*, vol. 2, pp. 1158–1163, Jul. 2003.

[14] M. Boerlage, R. Tousain, and M. Steinbuch, "Jerk derivative feedforward control for motion systems," in *Proc. Amer. Control Conf.*, 2004, pp. 4843–4848.

[15] T. Tang, H. Cai, Y. Huang, and G. Ren, "Combined line-of-sight error and angular position to generate feedforward control for a charge-coupled device–based tracking loop," *Opt. Eng.*, vol. 54, no. 10, Oct. 2015, Art. no. 105107.
[16] Q. He, Y. Luo, Y. Mao, and X. Zhou, "An acceleration feed-forward control method based on fusion of model output and sensor data," *Sensors Actuators A: Phys.*, vol. 284, pp. 186–193, Oct. 2018.
[17] I. B. Gonzalez *et al.*, "Fuzzy gain scheduled Smith predictor for temperature control in an industrial steel slab reheating furnace," *IEEE Latin Amer. Trans.*, vol. 14, no. 11, pp. 4439–4447, Nov. 2016.
[18] G. L. Raja and A. Ali, "Smith predictor based parallel cascade control strategy for unstable and integrating processes with large time delay," *J. Process Control*, vol. 52, pp. 57–65, Jan. 2017.
[19] T. Santos, B. C. Torrico, and J. E. Normey-Rico, "On the filtered smith predictor for MIMO processes with multiple time delays," *J. Process Control*, vol. 24, pp. 383–400, Mar. 2014.
[20] L. Sun, D. Li, Q. Zhong, and K. Y. Lee, "Control of a class of industrial processes with time delay based on a modified uncertainty and disturbance estimator," *IEEE Trans. Ind. Electron.*, vol. 63, no. 11, pp. 7018–7028, Nov. 2016.
[21] M. Sarkar, B. Subudhi, and S. Ghosh, "Unified Smith predictor based H∞ Wide-area damping controller to improve the control resiliency to communication failure," *IEEE/CAA J. Automatica Sinica*, vol. 7, no. 2, pp. 273–285, Mar. 2020.
[22] G. Lloyds Raja and A. Ali, "Enhanced tuning of Smith predictor based series cascaded control structure for integrating processes," *ISA Trans.*, vol. 114, pp. 191–205, Aug. 2021.
[23] S. Uma, M. Chidambaram, and A. Seshagiri Rao, "Set point weighted modified Smith predictor with PID filter controllers for non-minimum-phase (NMP) integrating processes," *Chem. Eng. Res. Des.*, vol. 88, pp. 592–601, May 2010.
[24] L. De Cicco, S. Mascolo, and S. Niculescu, "Robust stability analysis of Smith predictor-based congestion control algorithms for computer networks," *Automatica*, vol. 47, pp. 1685–1692, Mar. 2011.
[25] A. Batista and G. Fábio, "Performance improvement of an NCS closed over the internet with an adaptive Smith predictor," *Control Eng. Pract.*, vol. 71, pp. 34–43, Feb. 2018.
[26] Z. Cao, J. Chen, C. Deng, Y. Mao, and Z. Li, "Improved Smith predictor control for fast steering mirror system," *IOP Conf. Ser.: Earth Environ. Sci.*, vol. 69, no. 1, Jun. 2017, Art. no. 012085.
[27] Z. Hurk and M. Rezac, "Delay compensation in a dual-rate cascade visual servomechanism," in *Proc. 49th IEEE Conf. Decis. Control*, 2010, pp. 1639–1643.
[28] W. Ren *et al.*, "Stabilization control of electro-optical tracking system with fiber-optic gyroscope based on modified Smith predictor control scheme," *IEEE Sensors J.*, vol. 18, no. 19, pp. 8172–8178, Oct. 2018.
[29] L. Reggiani, L. Dossi, L. Barletta, and A. Spalvieri, "Extended Kalman filter for MIMO phase noise channels with independent oscillators," *IEEE Commun. Lett.*, vol. 22, no. 6, pp. 1200–1203, Jun. 2018.
[30] Z. Liu, Y. Li, Y. Wu, and S. He, "Formation control of non-holonomic unmanned ground vehicles via unscented Kalman filter-based sensor fusion approach," *ISA Trans.*, 2021, to be published, doi: 10.1016/j.isatra.2021.07.012.
[31] S. Wang, J. Feng, and C. K. Tse, "Analysis of the characteristic of the Kalman gain for 1-D chaotic maps in cubature Kalman filter," *IEEE Signal Process. Lett.*, vol. 20, no. 3, pp. 229–232, Mar. 2013.
[32] F. Auger, M. Hilairet, J. M. Guerrero, E. Monmasson, T. Orlowska-Kowalska, and S. Katsura, "Industrial applications of the Kalman filter: A review," *IEEE Trans. Ind. Electron.*, vol. 60, no. 12, pp. 5458–5471, Jun. 2013.
[33] B. Lima, D. Lima, and J. Normey-Rico, "A robust predictor for dead-time systems based on the Kalman filter," *IFAC-PapersOnLine*, vol. 51, no. 25, pp. 24–39, Jan. 2018.
[34] J. P. Helferty, "Improved tracking of maneuvering targets: The use of turn-rate distributions for acceleration modeling," *IEEE Trans. Aerosp. Electron. Syst.*, vol. 32, no. 4, pp. 1355–1361, Oct. 1996.
[35] J. Song, Z. Shi, B. Li, H. Wang, L. Han, and B. Du, "Analysis of influencing factors on fusion accuracy of virtual gyroscope technology and new data fusion method," *ISA Trans.*, vol. 100, pp. 422–435, Nov. 2019.
[36] X. Dong, X. Zhang, J. Zhao, M. Sun, and Q. Wu, "Multi-maneuvering sources DOA tracking with improved interactive multi-model multi-bernoulli filter for acoustic vector sensor (AVS) array," *IEEE Trans. Veh. Technol.*, vol. 70, no. 8, pp. 7825–7838, Aug. 2021.